Spectral Consequences of Periodic Orbit Bifurcations of AB_2 Stretching Vibrational Modes

T. Weston and M.S. Child
Physical and Theoretical Chemistry Laboratory,
South Parks Road, Oxford, OX1 3QZ

Abstract

Analysis of the kinetically coupled Morse oscillator model of Thiele and Wilson is used to relate abrupt changes in the qualitative character of the stretching vibrational spectra of AB_2 species to the loss of stability of the symmetric stretching periodic orbit above a certain energy threshold. A new uniform asymptotic solution of the relevant Hill's equation yields novel scaling relations that govern the dependence of the stability parameters on the mass ratio ($m_{\rm A}/m_{\rm B}$) and the reduced energy (E/D), scaled with respect to the dissociation energy. Crudely simulated dispersed emission spectra are used to illustrate the quantum mechanical consequences of the theory with particular reference to recent experiments on CS_2.

1 Introduction

The idea that changes in the classical phase space structure may be mirrored in the quantum mechanical spectrum is well demonstrated by semiclassical quantization techniques [1]. The existence of precessional and librational modes of the Henon-Heiles system [2] and coexistence of local and normal XH_n stretching modes [3] are particularly important examples. Less emphasis has been given to classical phase space bifurcations for heavy atom species, although the underlying classical mechanics for the stretching states of AB_2 molecules was elucidated by Thiele and Wilson [4] and later explored in relation to the onset of classical chaos by Matsushita and Terasaka [5].

Recent measurements of highly excited vibrational spectra of NO_2 [6] and CS_2 [7] suggest a reanalysis of the Thiele-Wilson model. Both spectra reveal a sharp transition from a readily assignable, orderly spectrum below a certain energy threshold to a severely congested unassignable one at higher energies. The complications in the case of NO_2 are probably due largely to vibronic interactions with a neighbouring electronic state [6], but the case of CS_2 is more puzzling. The low energy ($< 13000\text{cm}^{-1}$) spectrum, observed by dispersed emission, is analysed in terms of a strong bend/antisymmetric stretch Fermi resonance [7] with little or no evidence of antisymmetric stretch excitation.

Moreover the number of observed vibrational states rises quadratically with energy, as expected for two strongly coupled modes. Above the threshold however only statistical evidence of soft chaos can be extracted from the spectrum [7] and the rate of increase in the state count with energy acquires a new cubic component [7]. Evidently some sharp change in the system couples in states involving the antisymmetric stretching mode.

The argument of the present paper is that sharp changes of this type may be associated with changes in the stability of the symmetric stretching periodic orbit because such periodic orbit bifurcations are known to lead to new families of periodic orbits and ultimately chaotic regions of phase space [11]. The situation in the real molecule is complicated by Fermi resonance coupling to the bend but a full quantum mechanical study for a heavy atom species such as CS_2 is computationally prohibitive. The sudden onset of symmetric/antisymmetric stretch coupling arising from a change of periodic stability is however readily demonstrated in a stretching only model. Moreover the simplicities of the Thiele-Wilson model provide a global picture of the underlying classical mechanics of all AB_2 species, scaled with respect to the mass ratio $(m_{\mathrm{A}}/m_{\mathrm{B}})$ and the reduced energy expressed as a fraction of the dissociation energy (E/D).

The classical stability analysis proceeds by conventional linearisation about the symmetric stretching periodic orbit [8, 4], but the resulting Hill's equation is solved by a uniform asymptotic method, rather than the usual Mathieu equation approximation [4]. The new method has the advantage that it allows for strong anharmonicity in the symmetric stretching mode. Secondly it provides an analytical approximation for the monodromy matrix which is applicable at all energies - not simply at the bifurcation points. Finally the scaling properties allow separate identification of the influences of the mass ratio $(m_{\mathrm{A}}/m_{\mathrm{B}})$ and the reduced energy.

The Thiele-Wilson model is introduced in section 2 below, and the uniform asymptotic solution of the relevant Hill's equation is described in section 3. Aspects of the resulting symmetric stretch stability diagram are discussed in section 4. Section 5 illustrates quantum mechanical implications of these classical results by reference to CS_2. Finally the main conclusions are summarised in section 6.

2 The Thiele-Wilson model

The Thiele-Wilson model for AB_2 species employs a Hamiltonian of the form

$$H = \frac{(p_a^2 + p_b^2)}{2\mu_{AB}} + \frac{\cos\theta}{m_a} p_a p_b + D(1 - e^{-aq_a})^2 + D(1 - e^{-aq_b})^2 \qquad (1)$$

where $\mu_{AB} = m_A m_B/(m_A + m_B)$ and θ is the interbond angle. The realistic modelling of any particular species would clearly the inclusion of additional potential coupling terms but the above form has the advantage that it allows a scaling such that the classical stretching dynamics of all relevant species depends only on the reduced energy (E/D) and a single dimensionless coupling parameter

$$\lambda = \left[\frac{m_B}{m_A + m_B}\right] \cos\theta \tag{2}$$

Equation (1) also correctly allows the bonds to break and the spectroscopic evidence for non-hydride species is that the observed harmonic frequency ratios (ω_3/ω_1) (or ω_-/ω_+ in the notation of equation (7) below) are well reproduced by the effects of the $p_a p_b$ term in equation (1); for example the calculated frequency ratios for CO_2, CS_2, $HgCl_2$, NO_2, SO_2 and ClO_2 are (1.92, 2.52, 1.16, 1.48, 1.18 and 1.16) compared with (1.76, 2.33, 1.14, 1.24, 1.18 and 1.18) [9] after corrections to ω_1 for effects of Fermi resonance.

The scaling substitutions take the forms, for $\nu = a, b$

$$\begin{array}{ll} \tilde{q}_\nu = a q_\nu & \tilde{t} = \left(2a^2 D/\mu_{AB}\right)^{1/2} t \\ \tilde{p}_\nu = \left(2\mu_{AB} D\right)^{-1/2} p_\nu & \tilde{H} = H/2D \end{array} \tag{3}$$

in terms of which,

$$\tilde{H} = \frac{(\tilde{p}_a^2 + \tilde{p}_b^2)}{2} + \lambda \tilde{p}_a \tilde{p}_b + \frac{1}{2}\left(1 - e^{-\tilde{q}_a}\right)^2 + \frac{1}{2}\left(1 - e^{-\tilde{q}_b}\right)^2 \tag{4}$$

where λ is given by equation (2). Thus energies are expressed as fractions of the dissociations, $\epsilon = E/2D$ and times are related to the single bond harmonic frequency, $\omega_e = (2a^2 D/\mu_{AB})^{1/2}$.

It is convenient for what follows to transform to the symmetrised variables,

$$q_\pm = \tfrac{1}{\sqrt{2}}(\tilde{q}_1 \pm \tilde{q}_2) \quad p_\pm = \tfrac{1}{\sqrt{2}}(\tilde{p}_1 \pm \tilde{p}_2) \tag{5}$$

which casts equation (4) into the form

$$\tilde{H} = \frac{1}{2}(1+\lambda)p_+^2 + \frac{1}{2}(1-\lambda)p_-^2 + \frac{1}{2}\left(1 - \exp\left[-\frac{q_+ + q_-}{\sqrt{2}}\right]\right)^2 + \frac{1}{2}\left(1 - \exp\left[-\frac{q_+ - q_-}{\sqrt{2}}\right]\right)^2 \tag{6}$$

One then finds by expansion of the exponentials that the harmonic small amplitude frequencies are given in units of ω_e, by

$$\omega_\pm = \sqrt{1 \pm \lambda} \tag{7}$$

so that the coupling parameter λ is directly related to the frequency ratio by the equation,

$$\frac{\omega_-}{\omega_+} = \left(\frac{1-\lambda}{1+\lambda}\right)^{1/2} \tag{8}$$

3 Hill's equation: uniform asymptotic solution

The symmetric stretching mode, q_+, is governed according to equation (6) by the scaled Morse Hamiltonian

$$\tilde{H}_+ = \frac{1}{2}(1+\lambda)\,p_+^2 + \left(1 - e^{-q_+/\sqrt{2}}\right)^2 \tag{9}$$

from which it follows that $q_+(t)$ and p_+ vary as [1]

$$\begin{aligned} q_+(\tilde{t}) &= \sqrt{2}\ln\left[\frac{1+\sqrt{\epsilon}\cos\alpha_+(\tilde{t})}{1-\epsilon}\right] \\ p_+(\tilde{t}) &= -\sqrt{\frac{\epsilon(1-\epsilon)}{1+\lambda}}\frac{\sin\alpha_+(\tilde{t})}{1+\epsilon\cos\alpha_+(\tilde{t})} \end{aligned} \tag{10}$$

where ϵ is the reduced energy, $E/2D$ and $\alpha_+(\tilde{t})$ is the classical angle variable,

$$\alpha_+(\tilde{t}) = \sqrt{(1+\lambda)(1-\epsilon)}\tilde{t} + \alpha_+^0 \tag{11}$$

The reduction to Hill's equation, which governs the stability of this (q_+, p_+) motion, involves a linearisation for the transverse variables (q_-, p_-) about $q_- = p_- = 0$ under an effective Hamiltonian, with a time-dependence derived from equations (10). The necessary time derivatives implied by equation (6) are

$$\frac{\mathrm{d}q_-}{\mathrm{d}\tilde{t}} = \frac{\partial \tilde{H}}{\partial p_-} = (1-\lambda)p_- \tag{12}$$

and

$$\frac{\mathrm{d}p_-}{\mathrm{d}\tilde{t}} = -\frac{\partial \tilde{H}}{\partial q_-} \simeq -\left(\frac{\partial^2 \tilde{H}}{\partial q_-^2}\right)_{q_-=0} q_- \tag{13}$$

Alternatively, on combining equations (12) and (13)

$$\frac{\mathrm{d}^2 q_-}{\mathrm{d}\tilde{t}^2} = -(1-\lambda)\left(\frac{\partial^2 \tilde{H}}{\partial q_-^2}\right)_{q_-=0} q_- \tag{14}$$

It remains to evaluate $\frac{\partial^2 \tilde{H}}{\partial q_-^2}$ at $q_- = 0$ and to substitute for $q_+(\tilde{t})$ from equation (10). At the same time it is convenient to replace $\tilde{t}$ as the independent variable in equation (14) by $\alpha_+(\tilde{t})$ because α_+ increases by 2π for each cycle of the motion. The resulting Hill's equation - a second order linear equation in the periodic variable α_+ takes the form

$$\frac{\mathrm{d}^2 q_-}{\mathrm{d}\alpha_+^2} = -\omega^2(\alpha_+)q_- \tag{15}$$

where

$$\omega^2(\alpha_+) = \left(\frac{1-\lambda}{1+\lambda}\right)\left[\frac{1-2\epsilon-\sqrt{\epsilon}\cos\alpha_+}{\left(1+\sqrt{\epsilon}\cos\alpha_+\right)^2}\right] \tag{16}$$

The notation in equation (15) suggests a harmonic oscillator analogy, with a variable frequency $\omega(\alpha_+)$, but figure 1 shows that $\omega^2(\alpha_+)$ can become negative for $\epsilon > 0.25$ and α_+ values around zero, which correspond according to equation (10) to regions close to the outer turning point of q_+. The transverse variable q_- therefore tends to oscillate around zero in α_+ ranges where $\omega^2(\alpha_+) > 0$ and to diverge exponentially where $\omega^2(\alpha_+) < 0$. The stability or instability of q_+ depends on the relative influence of these two effects.

Equation (15) is mathematically analogous to the Schrödinger equation for a restricted rotor, with regions in which $\omega^2(\alpha_+) > 0$ and $\omega^2(\alpha_+) < 0$ corresponding to accessible and inaccessible ranges respectively. Cases in which $\omega^2(\alpha_+)$ is strictly sinusoidal therefore reduce to Mathieu's equation [10], but Fig 1 shows that $\omega^2(\alpha_+)$ is far from sinusoidal in the present situation. Instead equation (15) will be solved by the uniform asymptotic approximation of semiclassical mechanics [1].

The aim is to determine the monodromy matrix $\mathbf{M}$ [11] that relates the initial values of $q_-(\alpha_+^0)$ and $\dot{q}_-(\alpha_+^0)$ to their values at $\alpha_+^0 \pm 2\pi$, the most convenient initial value for present purposes being $\alpha_+^0 = -\pi$; thus

$$\begin{pmatrix} q_-(\pi) \\ \dot{q}_-(\pi) \end{pmatrix} = \mathbf{M} \begin{pmatrix} q_-(-\pi) \\ \dot{q}_-(-\pi) \end{pmatrix} \tag{17}$$

The stability properties of the (q_+, p_+) orbit depend on the eigenvalues of $\mathbf{M}$ [11], which are independent of the choice of α_+^0. Their product is necessarily unity because flux conservation requires that $\det \mathbf{M} = 1$. The present 2×2 case gives rise to three possibilities, which may be characterised by the value of trace($\mathbf{M}$) as follows:

$$\begin{array}{ll} \text{stable :} & -2 < \text{trace}(\mathbf{M}) = 2\cos\omega_\perp T < 2 \\ \text{unstable :} & \text{trace}(\mathbf{M}) = 2\cosh\gamma T > 2 \\ \text{unstable with reflection :} & \text{trace}(\mathbf{M}) = -2\cosh\gamma T < -2 \end{array} \tag{18}$$

Hence the trace has been parameterised by the orbit period, T, and a transverse frequency $\omega_\perp$ if the orbit is stable, or a Lyapunov exponent γ if it is unstable.

The method of solution of equation (16) is to represent $q_-(\alpha_+)$ in the "classically accessible" regions around $\alpha_+ = \pm\pi$ in the JWKB like form [1]

$$q_-(\alpha) = \omega^{-1/2}(\alpha) \left[A'_\pm \exp\left(i \int_{\pm\pi}^{\alpha} \omega \, d\alpha \right) + A''_\pm \exp\left(-i \int_{\pm\pi}^{\alpha} \omega \, d\alpha \right) \right] \tag{19}$$

where either upper or lower signs are taken throughout. The subscript on α_+ has been dropped for notational simplicity. The symmetry of equation (16) requires that $(d\omega_+/d\alpha) = 0$ at $\alpha_+ = \pm\pi$, from which it follows that,

$$\begin{pmatrix} q_-(\pm\pi) \\ \dot{q}_-(\pm\pi) \end{pmatrix} = \mathbf{W} \begin{pmatrix} A'_\pm \\ A''_\pm \end{pmatrix} \tag{20}$$

where

$$\mathbf{W} = \begin{pmatrix} \omega^{-1/2} & \omega^{-1/2} \\ i\omega^{1/2} & -i\omega^{1/2} \end{pmatrix} \tag{21}$$

Following the accepted semiclassical procedure [1] the required connections between the coefficients (A'_+, A''_+) valid for $\alpha \simeq \pi$ and (A'_-, A''_-) near $\alpha = -\pi$ are expressed in terms of two further matrices,

$$\mathbf{P} = \begin{pmatrix} e^{i\sigma/2} & 0 \\ 0 & e^{-i\sigma/2} \end{pmatrix} \tag{22}$$

and

$$\mathbf{T} = \begin{pmatrix} \sqrt{1+\kappa^2}e^{-i\phi} & -i\kappa \\ i\kappa & \sqrt{1+\kappa^2}e^{i\phi} \end{pmatrix} \tag{23}$$

where

$$\sigma = 2\int_{-\pi}^{-\alpha_1} \omega(\alpha)\, d\alpha = 2\int_{\alpha_1}^{\pi} \omega(\alpha)\, d\alpha \tag{24}$$

$$\kappa = e^{-\pi\beta} \tag{25}$$

$$\pi\beta = \begin{cases} -\int_{-\alpha_1}^{\alpha_1} \sqrt{-\omega^2}d\alpha & \epsilon > 0.25 \\ 0 & \epsilon = 0.25 \\ \int_{\alpha_1^*}^{\alpha_1} \omega d\alpha & \epsilon < 0.25 \end{cases} \tag{26}$$

$$\phi = \arg\left(\frac{1}{2} + i\beta\right) - \beta \ln|\beta| + \beta \tag{27}$$

The different choices of β depend on whether the roots of $\omega^2(\alpha) = 0$ are real or complex. It is readily verified from (16) that real roots, $\pm\alpha_1$ occur for $\epsilon > 0.25$ and that the roots are complex conjugates (α_1, α_1^*) for $\epsilon < 0.25$ and that $\alpha_1 = 0$ for $\epsilon = 0.25$.

The matrix $\mathbf{P}$ given by equation (22) takes into account phase changes to the coefficients in equation (19) arising from changes of the phase reference points from $\pm\pi$ to $\pm\alpha_1$ in Fig 1. The second matrix $\mathbf{T}$ incorporates approximate transmission and reflection coefficients associated with the "forbidden" region $-\alpha_1 < \alpha < \alpha_1$. Given the above forms, it follows by standard methods [1] that

$$A_+ = \mathbf{PTP}A_- \tag{28}$$

and hence by comparison with (17) and (19)

$$\mathbf{M} = \mathbf{WPTPW}^{-1} \tag{29}$$

Consequently $\det \mathbf{M} = 1$, as required by flux conservation, because $\det \mathbf{P} = \det \mathbf{T} = 1$ and $\det \mathbf{W}^{-1} = (\det \mathbf{W})^{-1}$. Finally the trace of $\mathbf{M}$ which determines the stability of the (q_+, p_+) orbit is given by

$$\mathrm{trace}\mathbf{M} = \mathrm{trace}\mathbf{P}^2\mathbf{T} = 2\sqrt{1+\kappa^2}\cos(\sigma - \phi) \tag{30}$$

because trace($\mathbf{ABC}$) = trace($\mathbf{CAB}$) etc.

Equation (30), which is the main new result, is particularly powerful in the present coupled Morse oscillator context because $\omega^2(\alpha_+)$ in equation (16) factorises into a molecule dependent factor $(1-\lambda)/(1+\lambda)$ and a term dependent only on the reduced energy, ϵ. The phase integrals, $\sigma(\epsilon,\lambda)$ and $\beta(\epsilon,\lambda)$ given by (24) and (26) therefore scale from one molecule to another according to the equations

$$\sigma(\epsilon,\lambda) = \sqrt{(1-\lambda)/(1+\lambda)}\sigma(\epsilon,0) \tag{31}$$
$$\beta(\epsilon,\lambda) = \sqrt{(1-\lambda)/(1+\lambda)}\beta(\epsilon,0) \tag{32}$$

It should be noted that $\sigma(\epsilon,0)$ takes the value of 2π at $\epsilon=0$ and falls smoothly to roughly $3\pi/2$ at the dissociation limit, $\epsilon=0.5$. $\beta(\epsilon,0)$ on the other hand is infinite at $\epsilon=0$ (hence according to (25), $\kappa=0$ in (30), takes positive values for $\epsilon<0.25$ and negative ones for $\epsilon>0.25$. The consequences of these variations of the stability or otherwise of the (q_+,p_+) orbit are discussed in the following section.

4 Symmetrical stretch stability diagram

As evidence of the implications of equations (30)- (31), Fig 2 shows the variations of trace($\mathbf{M}$) with ϵ for $\lambda=-0.45$ and $\lambda=-0.77$ In the first case the small values of λ ensures, via equation (31), a relatively slow variation of $\sigma(\epsilon,\lambda)$. The trace crosses the line trace($\mathbf{M}$) $=-2$ at $\epsilon\simeq0.12$ and $\epsilon\simeq0.34$ between which the symmetric stretching orbit is unstable with reflection. However $\epsilon<0.25$ in this range so that $\beta(\epsilon,\lambda)>0$ and $\kappa<1$ which means that trace($\mathbf{M}$) remains close to -2; consequently the Lyapunov exponent γ in (18) remains close to zero. At higher energies in Fig 2(a) the orbit remains stable with $-2<$ trace($\mathbf{M}$) <2. The higher value of λ relevant to Fig 2(b) ensures more rapid changes in $\sigma(\epsilon,\lambda)$ and to much larger values of the Lyapunov exponent than in the previous case. The dashed lines in Fig 2 were obtained by a trajectory based numerical determination of the trace [12]. Their proximity to the lines derived from equation (30) supports the validity of the uniform asymptotic approximation.

Notice also that the information in Fig 2 goes beyond that which is readily available by the Mathieu equation method [4]. The later is based on the recognition that the bifurcation conditions trace($\mathbf{M}$) $=\pm2$ correspond to

$$\mathbf{M}=\pm\mathbf{I} \tag{33}$$

where $\mathbf{I}$ is the unit matrix, which require periodic eigensolutions to equation (15) after one or two cycles. The bifurcation points are therefore equivalent to eigenvalues of the Mathieu equation provided that $\omega^2(\alpha_+)$ is approximately sinusoidal. The present approximation relaxes the sinusoidal condition and also yields analytical information in the stability frequency or Lyapunov exponent away from the bifurcation points.

For a global view of the results of the present analysis, Fig 3 shows the bifurcation diagram after one period of the symmetric stretch for all symmetric AB_2 species, plotted as a frequency ratio (ω_-/ω_+) and reduced energy, $\epsilon = E/2D$, phase diagram. The bifurcation line is marked as continuous if the transition is from stable to unstable (trace($\mathbf{M}$) $= 2$) and dashed if it is from stable to unstable with reflection (trace($\mathbf{M}$) $= -2$). The instability tongues correspond to $\omega_- : \omega_+ = n : 2$ anharmonic resonances, which converge at points on the horizontal axis because, in the notation of equation (30), $\beta \to \infty$ and $\sigma - \phi \to 2\pi$ as $\epsilon \to 0$. The forms of equations (25)-(26), (30) and the scaling relations (31) ensure that the tongues become extremely narrow for large ω_-/ω_+ and $\epsilon < 0.25$ because β becomes positive and the Lyapunov exponents increase rapidly with (ω_-/ω_+) for given ϵ. Consequential changes in the quantum mechanical spectrum are therefore predicted to occur more abruptly for species with larger (ω_-/ω_+) ratios. Arrows are used to indicate the theoretical (ω_-/ω_+) values for selected molecules, as given by equations (2) and (8).

5 Quantum mechanical implications for CS_2

The molecule CS_2 is of particular interest, first because of the experimental results [7] that were summarised in the introduction. Secondly it has the highest frequency ratio (ω_-/ω_+) in Fig. 3; hence, according to the previous discussion, it is predicted to show the most abrupt change in its stretching vibrational dynamics.

To simulate a relevant quantum mechanical spectrum the stretching states were modelled by diagonalising the quantum equivalent of equation (1) in a symmetrized Morse product basis.

From equation (9) the pure symmetric stretch eigenenergies can be written as,

$$E(n) = 2D\,(1+\lambda)^{1/2}\,\tilde{\hbar}(n+1/2) - \frac{1}{4}D\,(1+\lambda)\,\tilde{\hbar}^2(n+1/2)^2 \qquad (34)$$

where $\tilde{\hbar} = \left(a^2/2D\mu_{AB}\right)^{1/2}\hbar$ is the dimensionless Planck's constant in the scaled units derived in (3). For the above equation, it is evident that this quantity can be estimated from the experimental symmetric stretch frequency and anharmonicity, which are 672.51cm^{-1} and -1.2372cm^{-1}respectively [13], as,

$$\tilde{\hbar} = \frac{4}{(1+\lambda)^{1/2}}\frac{(-x_{11})}{\omega_1} \simeq 0.01412 \qquad (35)$$

This leads to an estimate of the dissociation energy (D) of 45586cm^{-1} or 5.65eV which is in rough agreement with a direct experimental value of 5.60eV [14]. Using this value of $\tilde{\hbar}$ the each oscillator contains $\text{int}(1/\tilde{\hbar} - 1/2) = 70$ bound states and the Hamiltonian factorises into two 2500×2500 blocks.

Two estimates of the parameter λ were considered, according to whether equation (2) or equation (8) is employed, the former gives $\lambda = -0.7272$ and the latter $\lambda = -0.6858$. For reasons discussed below the mean value $\lambda = -0.7065$ was adopted.

Within the constraints of the present stretching only model the conditions of the dispersed emission experiment were simulated by assuming an initial wavepacket of variable energy in the q_+ (or ν_1) mode and only zero-point excitation in the antisymmetric stretch q_- (or ν_3). The question is whether or not the variational eigenfunctions at different energies do or do not retain similar selectivity with respect to the q_- (or ν_3) mode.

The results in Fig 4 show a strong q_+ (or ν_1) progression for an initial wavepacket with a mean energy of $\bar{\epsilon} = 0.15$ in scaled units or 13676cm^{-1}. The spread of the wavepacket barely reaches the bifurcation point at $\bar{\epsilon} = 0.23$ or 20970cm^{-1} at which the symmetric stretch periodic orbit becomes unstable but there is an additional weak "period doubling structure" from about $\epsilon = 0.15$ or 13676cm^{-1}, the origin of which is discussed below. At the higher mean energy of $\bar{\epsilon} = 0.25$ or 22793cm^{-1} there is an abrupt change in the density of spectral lines in Fig. 4(b) the onset of which correlates well with the loss of stability for the symmetric stretching orbit at $\epsilon = 0.23$ or 20970cm^{-1}.

The contention that the character of the quantum mechanical spectrum is strongly influenced by the stability or otherwise is well supported by the above results. The situation with respect to the experimental spectrum of CS_2 is however more complicated because the measurements indicate a loss of order at about 13000cm^{-1}, which is well below the calculated transition at around 20970cm^{-1} in Fig. 4(b). It seems more likely therefore that the observed change in character is related to the weak additional structure in Fig. 4(a), which is associated with the strongest of the sequence of high order resonances, whose onset energies are predicted by Fig. 5. The diagram is analogous to the trace plots in Fig. 2 except that the vertical scale is presented as a frequency ratio ($\omega_\perp/\omega_\parallel = \omega_\perp T/2\pi$) using the notation of equation (31). Related classical studies show that most of the predicted resonances are very weak, apart from the 9:4 resonance which retains a significant island of stability over the energy range of the weak feature in Fig. 4(a). Each 9:4 periodic orbit has four times the period of the symmetric stretch, which would argue for eigenvalues at 0.25 times the basic spacing but only alternate ones have the correct symmetry to appear in Fig. 4, which accounts for the apparent period doubling. In addition the 9:4 character of the associated eigenfunctions is clearly apparent from Husimi phase projections [12].

The steep slope of the frequency ratio plot in Fig. 5 makes the onset of the 9:4 resonance quite sensitive to the choice of λ, and the above choice of λ as the mean between the values given by equations (2) and (8) was inspired by the observed change in the spectral character at around 13000cm^{-1}. The calculated period doubling feature would start respectively at 19146cm^{-1} and 7294cm^{-1} for $\lambda = -0.7272$ as given by equation (2) and $\lambda = -0.6858$ consistent with equation (8).

6 Conclusions

The connection between the loss of periodic orbit stability and abrupt changes in the quantum dynamics of AB_2 stretching states, in the context of the kinetically coupled Morse oscillator model of Thiele and Wilson.

A new uniform asymptotic solution to the relevant Hill's equation was used to obtain analytical formulae for the global dependence of the symmetric stretching orbit stability parameters as function of the reduced energy (E/D) and of the frequency ratio (ω_-/ω_+) (or ω_3/ω_1) of different species. The scaling properties of the resulting equations led to the prediction of an increasingly abrupt energy dependence of the Lyapunov exponent for increasingly large frequency ratios (ω_-/ω_+).

Quantum mechanical studies modelled on the stretching states of CS_2 were used to shed light on a known abrupt change in the character of the dispersed emission spectrum. A crudely simulated stretching only spectrum contained a simple progression in ω_1 at energies over which ν_1 was stable but a much more complicated spectrum indicative of strong stretch-stretch coupling at energies above the ν_1 instability threshold.

References

[1] M. S. Child, Semiclassical Mechanics with Molecular Applications, (Oxford University Press, 1991)

[2] D. W. Noid, M. L. Kosykowski and R. A. Marcus, J. Chem. Phys. **71** (1979) 2864

[3] M. S. Child and L. Halonen, Adv. Chem. Phys. **57** (1984), 1

[4] E. Thiele and D. J. Wilson, J. Chem. Phys. **35** (1961) 1256

[5] T. Matsushita and T. Terasaka, Chem. Phys. Lett. **100** (1983) 138

[6] R. Georges, A. Delon and R. Jost, J. Chem. Phys. **103** (1995) 1732

[7] G. Sitja and J.P. Pique, Phys. Rev. Lett. **73** (1994) 232

[8] G. W. Hill, Acta Math. **8** (1886) 1

[9] G. Herzberg, Electronic Structure of Polyatomic Molecules (van Nostrand, 1967)

[10] M. Abramowitz and I. A. Stegun, Handbook of Mathematical Functions (Dover, 1965)

[11] M. Tabor, Chaos and Integrability in Nonlinear Dynamics (Wiley Interscience, 1989)

[12] T. Weston, D.Phil thesis (Oxford University, 1996)

[13] G. Sitja, H. Ring, J. P. Pique, G. Chambaud, P. Rosmus, unpublished.

[14] J. Fournier, C. Lalo, J. Deson and C. Vermeil, J. Chem. Phys. **66** (1977) 2656

Figures

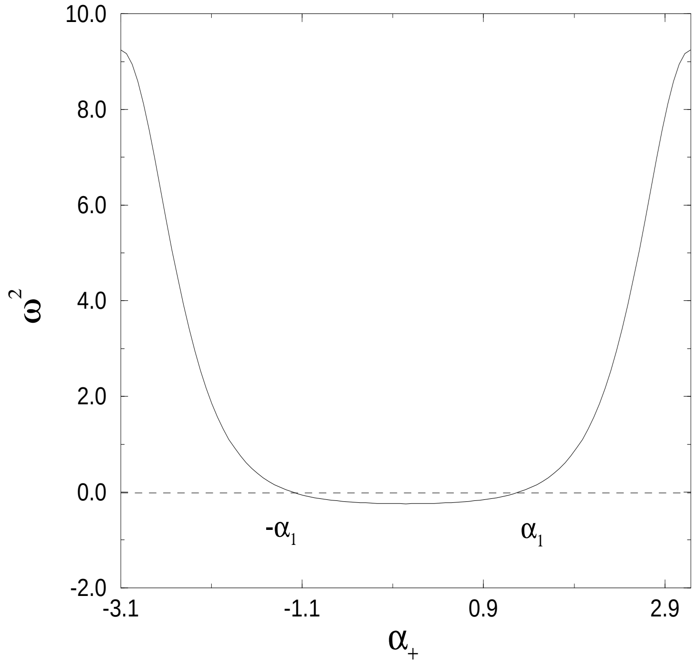

Figure 1: Variation of ω^2 with α_+ for $\epsilon = 0.4$ and $\lambda = -0.2$

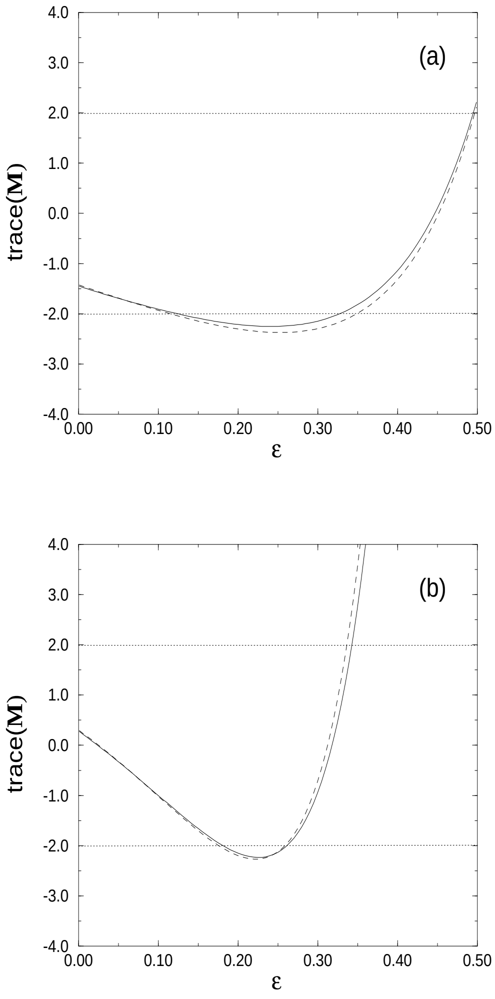

Figure 2: Reduced energy dependencies of trace($\mathbf{M}$) for (a) $\lambda = -0.45$ and (b) $\lambda = -0.77$. Present asymptotic results, shown by the continuous lines, are compared with numerical results, indicated by the dashed lines.

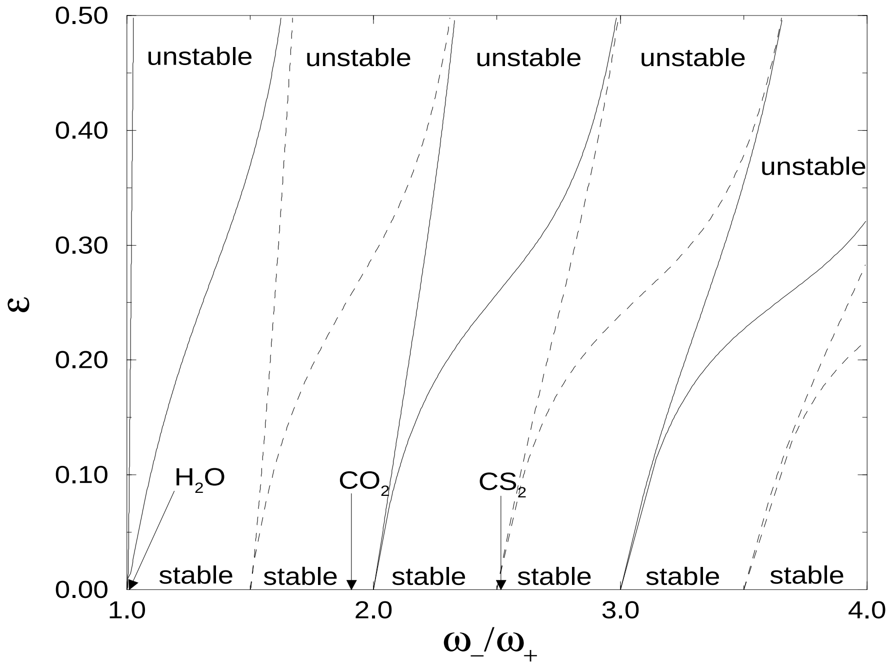

Figure 3: The symmetric stretch stability diagram expressed in terms of dimensionless frequency ratio and reduced energy variables. Continuous lines indicate bifurcation from stable to unstable character (trace($\mathbf{M}$) = 2) at an n : 1 resonance with $n = 1, 2$ and 3 from left to right. Dashed lines represent similar bifurcations to motions that are unstable with reflection (trace($\mathbf{M}$) = -2) at $(2n+1)$: 2 resonances, again with $n = 1, 2$ and 3. Arrows indicate the positions of various molecules, as determined by equations (2) and (8)

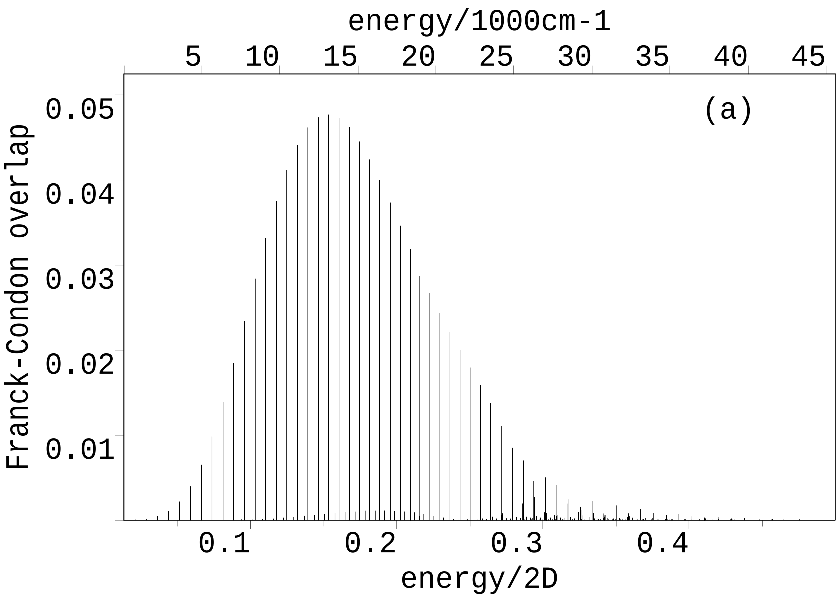

energy/1000cm-1
5
10
15
20
25
30
35
40
45
(a)
Franck-Condon overlap
0.05
0.04
0.03
0.02
0.01
0.1
0.2
0.3
0.4
energy/2D

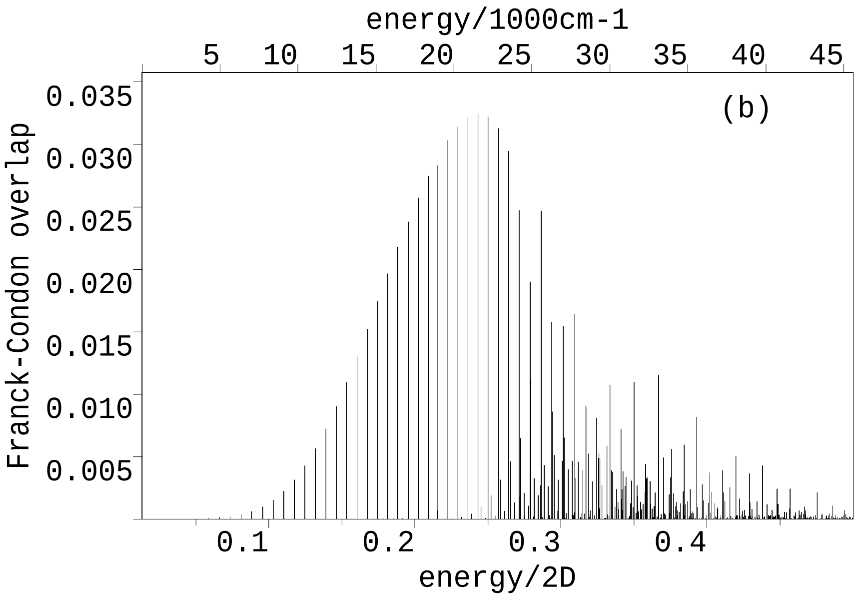

Figure 4: Franck-Condon overlap intensities between $v_{-} = 0$ (or $v_3 = 0$) wavepackets and the quantum mechanical eigenstates for a model of the stretching modes of CS_2 with parameters $\lambda = -0.7065$, $\omega_e = 1193\mathrm{cm}^{-1}$ and $D = 45586\mathrm{cm}^{-1}$. Results are shown for two mean reduced energies (a)$\bar{\epsilon} = 0.15$ and (b)$\bar{\epsilon} = 0.25$, which bracket the bifurcation energy at $\epsilon = 0.21$.

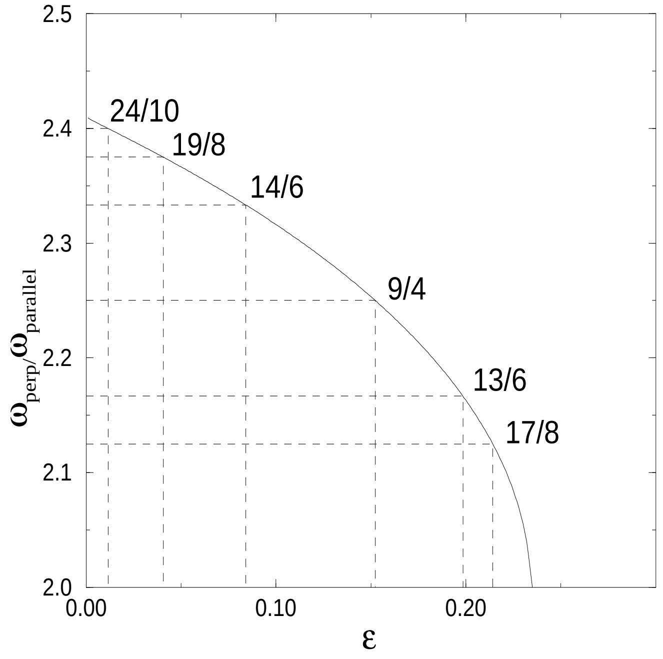

Figure 5: Predicted bifurcations (or anharmonic resonances) prior to the symmetric stretching instability for the CS_2 model. The frequency ratio ($\omega_\perp/\omega_\parallel$) is related to the trace in equation (18) by the formula $\omega_\perp/\omega_\parallel = \omega_\perp T/2\pi$